RESEARCH PAPER

Enhanced Photocatalytic Degradation of 4-chlorophenol using Lanthanum Oxide Nano-particles under UVC/Vis Irradiation

Zeinab Ghaedrahmat [1], Seyedeh Maryam Moussavi [2], Sahand Jorfi [2,3], Mehrnoosh Abtahi Mohasel [4], Neamat Jaafarzadeh [2,3,5]*

[1]*Department of Environmental Health Engineering, shoushtar Faculty of Medical Sciences, Shoushtar, Iran*

[2] *Department of Environmental Health Engineering, School of Health, Ahvaz Jundishapur University of Medical Sciences, Ahvaz, Iran*

[3] *Environmental Technologies Research Center, Ahvaz Jundishapur University of Medical Sciences, Ahvaz, Iran*

[4] *Environmental and Occupational Hazards Control Research Center, Shahid Beheshti University of Medical Sciences, Tehran, Iran*

[5] *Department of Environmental Health Engineering, School of Public Health, Shahid Beheshti University of Medical Sciences, Tehran, Iran*

ARTICLE INFO

Article History:
Received 29 July 2020
Accepted 18 October 2020
Published 01 January 2021

Keywords:
4-chlorophenol
Lanthanum oxide
Photocatalytic oxidation
UVC radiation
Visible radiation

ABSTRACT

Photocatalytic oxidation using novel photo-catalysts has been considered as an effective method for destruction of recalcitrant organics. In this study, photocatalytic degradation of 4-chlorophenol (4-CP) using lanthanum Oxide nanoparticles (LONPs) was investigated under UVC/Vis irradiation. Effect of operational parameters including pH (2 – 11), catalyst content (250-3000 mg L^{-1}), contact time (20 - 180 min) 4-CP concentration (25- 400 mgL^{-1}) were investigated according to one factor at the time experimental procedure. Highest removal efficiency of 4-CP was observed at pH =7. Result was indicated that the removal of 4-CP was increased from 76% to 92%, with increasing catalyst dosage from 0.25 to 1 g L^{-1}. Then, a decrease was observed in 4-CP removal with an enhancement in catalyst dosage from 1 to 3 g L^{-1}. Highest 4-CP removal (98%) was observed at the initial concentration of 25 mg L^{-1}. At the contact time from 20 to 60 min, removal efficiency of 4-CP was increased from 24% to 64%, respectively. The contact time was increased to 120 min, removal efficiency of 4-CP was increased to 100%. Therefore, the optimal reaction time was 100 min. The AOS indices was showed an increasing trend of mineralization. In other words, the process of degradation of 4-CP was improved with photocatalytic degradation by UVC-La_2O_3. Among the kinetic models, the pseudo-first order model due to the highest correlation coefficient of R^2 = 0.991 for the La_2O_3-UVC process.

How to cite this article
Ghaedrahmat Z., Moussavi S.M., Jorfi S., Abtahi Mohasel M., Jaafarzadeh N. Enhanced Photocatalytic Degradation of 4-chlorophenol using Lanthanum Oxide Nano-particles under UVC/Vis Irradiation. J Nanostruct, 2021; 11(1): 165-180. DOI: 10.22052/JNS.2021.01.018

INTRODUCTION

The 4-Chlorophenol has been identified as a harmful chemical to the environment and living beings even at very low concentrations. Because of its irresolvability in the environment and also due to properties such as carcinogenicity, mutagenicity and toxic effects of chronic, 4-CP are primarily considered as pollutants by the American Environmental Protection Agency and European Union [1]. The 4-CP with the chemical formula of C_6H_5ClO is one of the types of 4-CP in which hydrogen No. 4 is substitute with chloride

* *Corresponding Author Email: n.jaafarzade@yahoo.com*

on the benzene ring of phenol [2]. The 4-CP is found in large-scale in several industries such as fungicides, herbicides and microbicides, pulp and paper industries, wood preservation, disinfection materials, sulfur and nitrogen from coal, as a combination intermediates in the synthesis of dyes and medicine, denatured alcohol, as a solvent in the oil refining, petrochemical, manufacturing pesticides, anti-microbial agents, and it is also used in production of drugs [3, 4]. The concentrations of 4-CP have been reported in effluent of these industries in the range of 50 to 400 mg L^{-1} [4]. European Union has determined a limit of 0.1 µg L^{-1} and 0.5 µg L^{-1}, respectively, as the maximum levels of pesticides and their breakdown products in the environment [5]. Advanced oxidation processes including photocatalytic degradation are considered as an efficient methods for removal of recalcitrant organics such as Ultrasonic/Fenton, integrating technology of oxidation and sonication, combination of absorption and oxidation, combination of optical dispersion of photo-catalyst (titanium dioxide) and etc.[6-13]. But in the most cases, these methods are not efficient in the case of destruction of low concentration of organics or not being cost effective [6]. Photocatalytic methods have greater interest due to the nature of their processes, such as ability for degradation of a wide range of contaminants, high mineralization potential, being non-toxic, non-corrosive and harmless for the environment [14-17]. The most widely used photo-catalyst include semiconductors such as TiO_2, ZnO, CdS, ZrO_2, WO_3, SnO_2 which have been used for photocatalytic oxidations. Many semiconductors (ZnO, $CdSSnO_2$) or (ZrO_2, SnO_2) have a photo corrosive nature and higher band gap energy [18, 19]. On the other hand, the low level of mineralization and need for the final filtration stage, high recombination rate of electrons and holes are produced by the edge of the absorption in the ultraviolet area (that causing its photocatalytic activity to be insignificant in visible light), are limits practical applications of these semiconductors. Thus, these compounds cannot be efficient photo-catalyst for long-term use [20-23]. In recent years, the use of lanthanum oxide have been increased because of its use as piezoelectric materials, thermoelectric materials, catalyst support and important component manufacturer convectors of exhaust car-received [24]. In addition, industrial applications such as wastewater treatment, water treatment has also been reported for these metal oxides [14, 25-27]. In this research, nano particles of lanthanum oxide were synthesized using water as an environmentally benign solvent and starch as a capsulating agent. The starch in the solution mixture prevents the use of organic solvents that are relatively harmful. The aim of the present study was to determine the removal efficiency of 4-CP from aqueous solutions using lanthanum oxide under UVC/Vis radiation.

MATERIALS AND METHODS

Chemicals

All chemical were analytical grad and used without further purification, which included 4-chlorophenol (C_6H_5ClO, Sigma-Aldrich, 98%), sulfuric acid (H_2SO_4, Sigma-Aldrich, 98%), and sodium hydroxide (NaOH, Sigma-Aldrich, 99 %), lanthanum nitrate (La $(NO_3)_3$), Sigma-Aldrich, 99.99%), Starch ($(C_6H_5O_{10})_n$, Merck, 99%).

Synthesis of nano lanthanum oxide

2.5 g of starch was dissolved in 100 ml of water for nano lanthanum oxide synthesis. Then 0.1 M lanthanum nitrate was applied to some starch solution amounts, so that the ratio of starch: lanthanum nitrate was 1:1. The solution was stirred for 30 min, evaporated at 100 °C to dryness and calcinated for 2 hours at 400, 600 and 800 °C [28].

Photocatalytic Assessment

The efficiency of the photocatalysts was investigated as a target pollutant through the degradation of 4-CP. The experiments were carried out in a photo-reactor with a (30mm × 4mm × 4mm), with magnetic stirring (MR 3001 K, Heidolph). Photo-reactor system of UVC/La_2O_3 used in this study was surrounded by a water shell chamber to control the temperature during the reaction. As a light source, two UVC lamps were used with a wavelength centered at 254 nm (Philips, TUV 8W/G5 T5) and a metallic cover was put outside to separate other light sources. (Fig. 1). The solar experiments took place with a xenon lamp. Various quantities of catalysts were added to the aqueous solution containing 4-CP in both irradiation conditions. To determine the adsorption and desorption necessary for balance, the solution was stirred for 30 minutes without illumination. The reaction temperature was kept at 20–25 °C. By adding 0.1 N H_2SO_4 or NaOH and

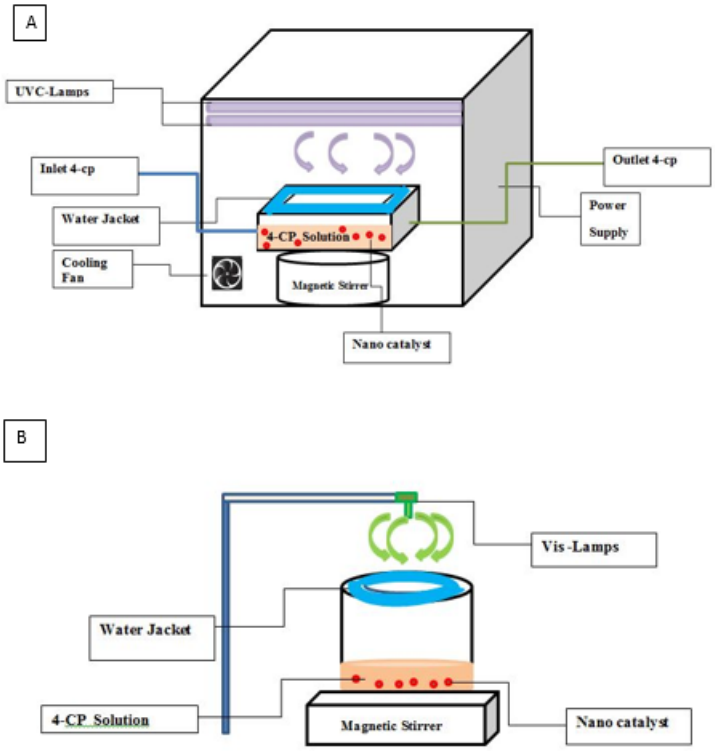

Fig. 1. Schematic diagram of (a) UVC/La_2O_3 photo-reactor, (b) Visible/La_2O_3

monitoring with a digital pH meter, the pH solution was changed (Jenway 3510).

5 mL of suspension was regularly removed from the reactor during all the experiments. Photocatalysts were isolated by centrifugation (PIT320, Universal) and the resulting transparent solution was examined at the 4-CP maximum wavelength (λmax,4-CP = 279 nm) using UV spectroscopy (UV2100, Unico).

The parameters are influencing the removal of 4-CP, included pH, catalyst dosage, contact time, initial concentration of 4-CP [4, 9, 14, 25, 29-31]. The synthetic samples were prepared by 4-CP stoke solution (1000 mg L^{-1}). In the first step, effect of pH was investigated in the range of 2 to 11 [10, 31]. Sodium hydroxide and Acid hydrochloric acid were used to adjust the pH. Afterwards, taking into account the optimum pH value, effect of catalyst dosage in the range of 250-3000 mg L^{-1} [14, 25, 29], contact time in the range was 20 to 180 min [9] and 4-CP concentration (25 to 400 mg L^{-1}) [5, 10, 29, 31] were studied. Mineralization of 4-CP were also investigated.

Characterization

The catalyst surface morphology analysis was conducted using scanning electron microscopy (SEM, Tescan, Mira3, Czech Republic). Images were taken with a 30 kV accelerating voltage and a 30 mA applied current. Each CDT SEM image was then used to calculate the samples' pore diameter size distribution (using Measure IT and Nano Measurement software).

RESULTS AND DISCUSSION

Characterization of LONPs

The particle size and morphology of LONPs were studied with scanning electron microscopy (FE-SEM) (Fig. 2). The particle size of LONPs were 25-38 nm. Using FESEM at different magnification and also its particle diameter displays, the grain size, shape and surface properties such as morphology were observed. It indicates that the particles are agglomerated.

Fig. 3a shows that the TEM image of La_2O_3. The agglomerated sample within the Nano range is seen in the TEM analysis. It has been found from TEM analysis that the particles of the samples are shapeless due to extreme agglomeration. However, to say that the particles collected are nano particles, the particles are far below the nanometer scale.

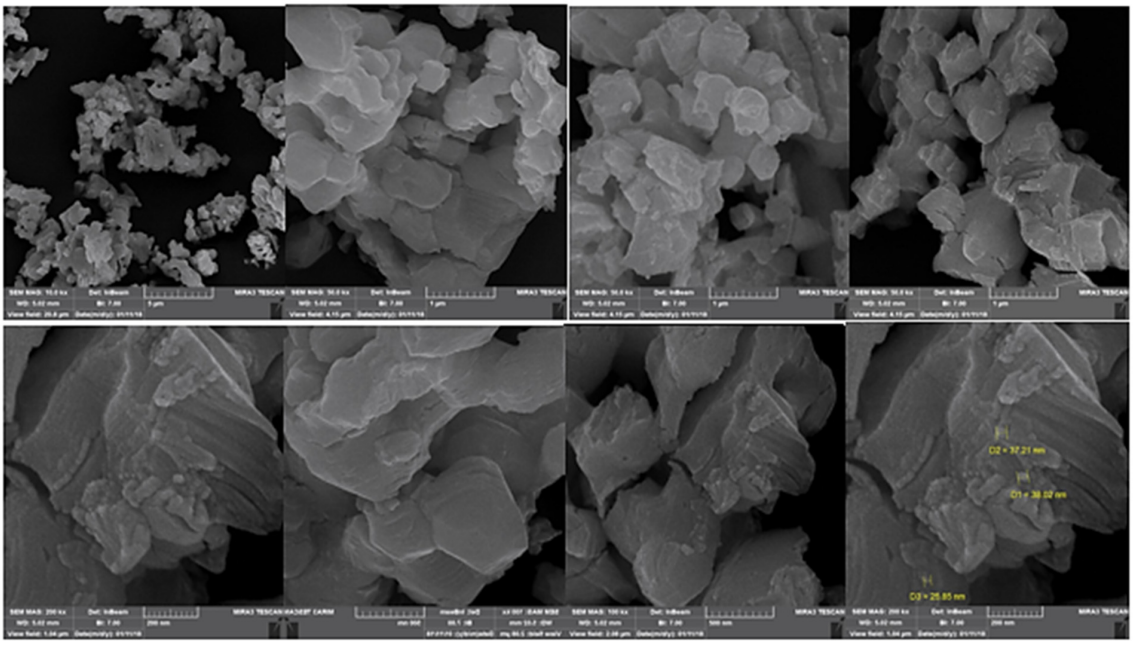

Fig. 2. FESEM images of LONPs

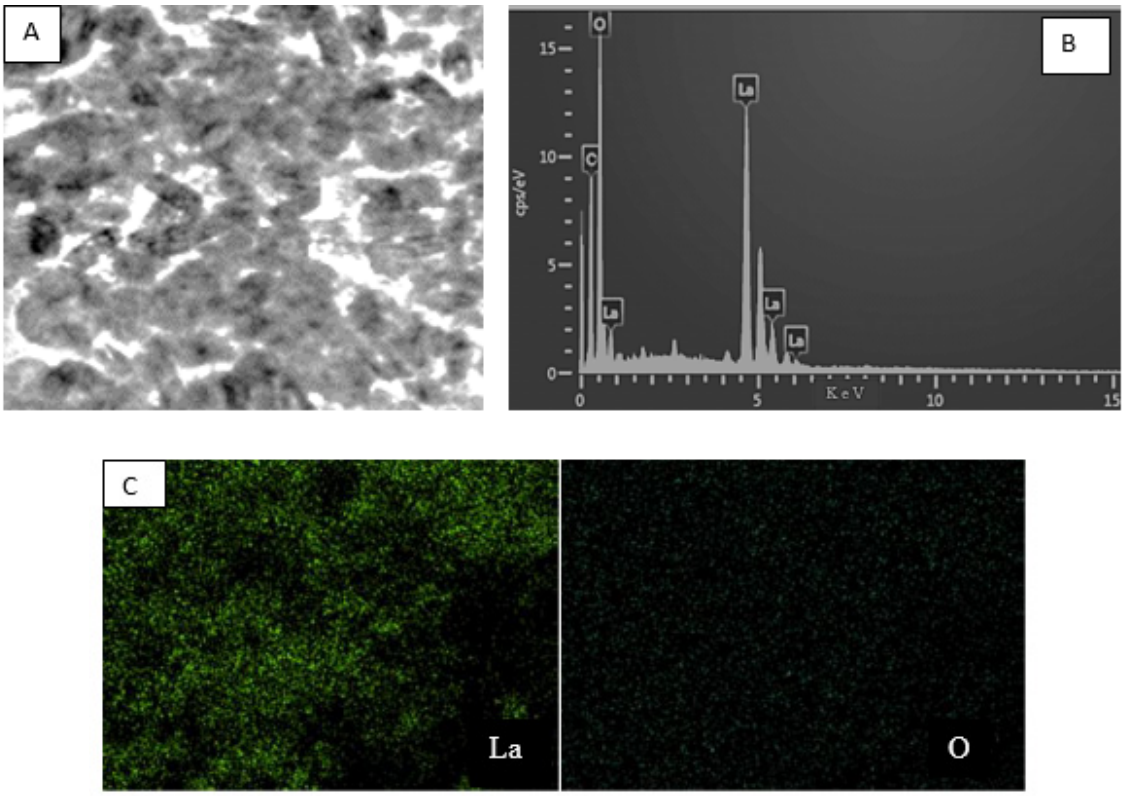

Fig. 3. (a) TEM image of LONPs, (b) EDS spectrum of LONPs, (c) Map of LONPs

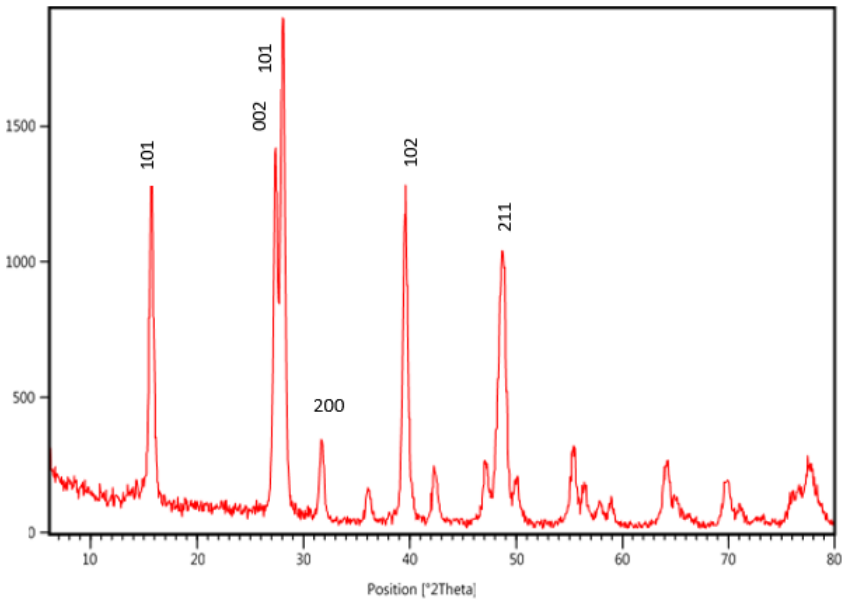

Fig. 4. XRD pattern of LONPs

EDAX analysis studied the chemical purity and stoichiometry of the La_2O_3 sample. Fig. 3b gives the energy repulsive spectrum of precipitated La_2O_3. The EDAX analysis indicates that both La and O are present in the synthesized La_2O_3. X-Ray mapping results have also been obtained, showing the distribution of all the microstructure elements present.

The Elemental X-Ray mapping of La_2O_3 samples is shown in Fig. 3c. Elemental X-ray mapping shows that the image of the spherically porous microstructure was observed in La_2O_3. Oxygen is rich in the matrix (57 %) and lanthanum is unequally distributed (43 %).

Fig. 4 shows the X-ray diffraction (XRD) patterns average crystalline size of LONPs**.** According to Fig. 4, the XRD patterns had peaks at 15.7°, 27.3°, 28°, 30.7°, 31.7°, 36.11°, 39.11°, 42.3°, 47.1°, 48.9°, 50°, 55.4°,56.4°, 57.86°, 58.8°, 64.2°, 69.7°, 71.1°, 72.8°, 55.8°, 77.6° by scanning in angular range (2Θ) from 10 to 80°. The 4 diffraction sharp peaks at 2ϑ =15.9°, 27.328.1°, 39.65°, 49.23° which is corresponding to (1 0 0), (0 0 2), (1 0 1), (2 1 1). This is in good agreement with the findings of littrature for the La_2O_3 [32]. The hexagonal step formation for La_2O_3 was confirmed by the XRD patterns acquired in the present analysis. The diffraction peaks (200) and (211) found in Fig. 4 were due to the small amount of La $(OH)_3$ in the La_2O_3 powder [32, 33]. This is in good agreement with the standard Joint Committee on Powder Diffraction Standards card No: 50-0602. The extended peaks, are well illustrated polycrystalline properties, and size reduction of nanoparticles La_2O_3. The average crystallite size of anatase in the different samples can be evaluated by using the Debye-Scherrer formula on the main peak for anatase (2θ =28.1°):

$$D = 0.9\lambda / \beta \cos\theta \quad (1)$$

where D is the average crystallite size, K the constant which is taken as 0.89 here, λ the wavelength of the X-ray radiation (λ=1.5418A^0), β the corrected band broadening (full width at half maximum (FWHM) after subtraction of equipment broadening, and ϑ is the diffraction angle [34]. The average crystallite size was calculated 237nm.

The FTIR spectrum of La_2O_3 nanoparticles obtained in the number of waves of 500 to 4000 is shown in Fig. 5. As you can see, Fig. 5 indicates the FTIR spectra of LONPs including bands at 477.34, 644.09, 1465.25, 1640.25, 2354.98, 2924.3, 3447.64, 3607.35, 3791.22 cm^{-1}. The peak corresponding to the (La-O) observed at 477 cm^{-1} indicates the development of lanthanum oxide. The absorption band at 644 cm^{-1} reflects the stretching of metal-oxygen (La-O stretch), confirming the development of nanoparticles of La_2O_3. At 1640 cm^{-1}, the corresponding (OH) bending mode is observed. The water and

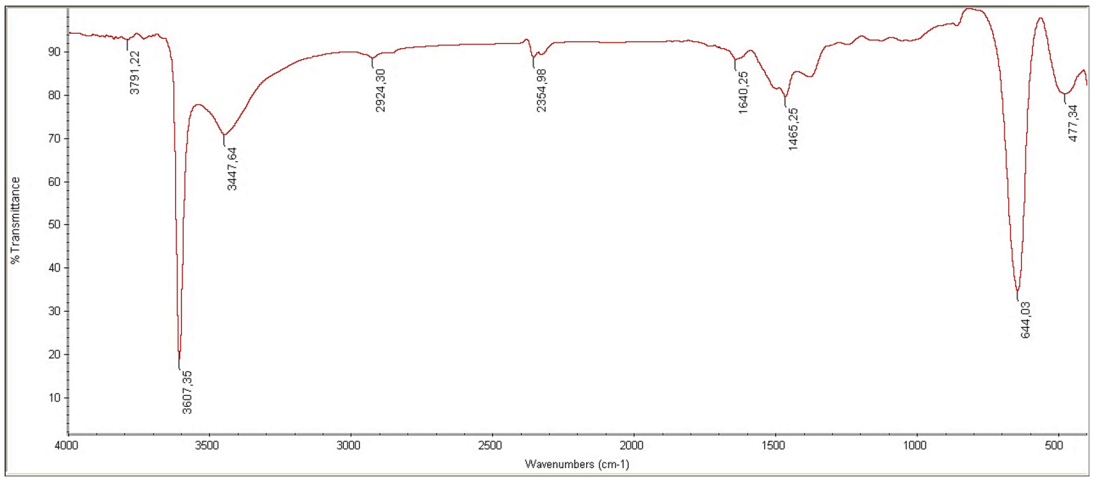

Fig. 5. FTIR spectra of LONPs

Table 1. Functional groups determined by FTIR analysis

Wavelength (cm^{-1})	Functional group
477	La-O
644	La-O stretch
1640	OH
3440	O-H stretching
3607	O-H stretching
3790	O-H stretching
2354	CO_2
2924	C-H

hydroxyl stretches (O-H stretching) are assigned to absorption bands at 3440, 3607 and 3790 cm^{-1}. From the absorption of atmospheric CO_2, the band at 2354 cm^{-1} can emerge. In terms of C-H bonding, the bands observed at 2924 cm^{-1} are present (Table 1). The hydrophilic character of lanthanum oxide and its affinity with carbon dioxide are shown by FTIR analysis.

The area of the BET surface and the pore size distribution of LONPs were also studied. The surface areas of the specimens were evaluated using N_2 adsorption-desorption isotherms at 77 K, with a Belsorp-mini II adsorption apparatus based on Brunauer-Emmett- Teller (BET) theory (Table 2). The isotherm was indicated high adsorption at P/P_0 = 0.99. The BET surface area was found to be 3.7936 m^2g^{-1}.

Photocatalytic oxidation

Effect of pH

The effect of pH in the range of 2-11 on removal efficiency was studied at catalyst dosage of 1500-3000 mg L^{-1}, contact time= 100 min and initial 4-CP concentration of 25 mg L^{-1} (Fig. 6). Result indicate that the 4-CP was rapidly degraded at pH =7. Indeed, the removal of 4-CP was approximately achieved after 100 min at pH=7. While, around 88.6, 68.21, 64.14, 60.7 and 40.61 % of 4-CP were degraded at pH 8, 9, 10 and 11, respectively. Then, a decrease was observed in 4-CP removal with an enhancement in pH in the range of alkaline conditions [8, 20]. This result is consistent with other studies [5, 7, 35-43]. At higher pH, the OH^- in the solution was increase and compete with 4-chlorophenol and reduce the process efficiency. On the other hand, at lower pH, H^+ was increased. Since at lower pH, 4-Chlorophenol is present in ions, protons are compete with 4-chlorophenol ions. This finding was in accordance with previous studies [43-45].

Effect of LONPs dosage

The effect of the catalyst dosage in the range of 250- 3000 mg L^{-1} was studied at pH = 7, contact time= 100 min and initial 4-CP concentration of 25 mg L^{-1} (Fig. 7). Result was indicated that the

Table 2. BET surface area, pore volume, pore diameter of the La_2O_3

BET plot		
V_m	0.8716	[cm^3(STP) g^{-1}]
$a_{s,BET}$	3.7936	[m^2 g^{-1}]
C	164.74	
Total pore volume(p/p_0=0.990)	0.023208	[cm^3 g^{-1}]
Mean pore diameter	24.47	[nm]
Langmuir plot		
Vm	1.1963	[cm^3(STP) g^{-1}]
$a_{s,Lang}$	5.207	[m^2 g^{-1}]
B	0.4385	
t plot		
Plot data	Adsorption branch	
a_1	3.5477	[m^2 g^{-1}]
V_1	0	[cm^3 g^{-1}]
BJH plot		
Plot data	Adsorption branch	
V_p	0.023308	[cm^3 g^{-1}]
$r_{p,peak}$(*Area*)	1.72	[nm]
a_p	3.855	[m^2 g^{-1}]

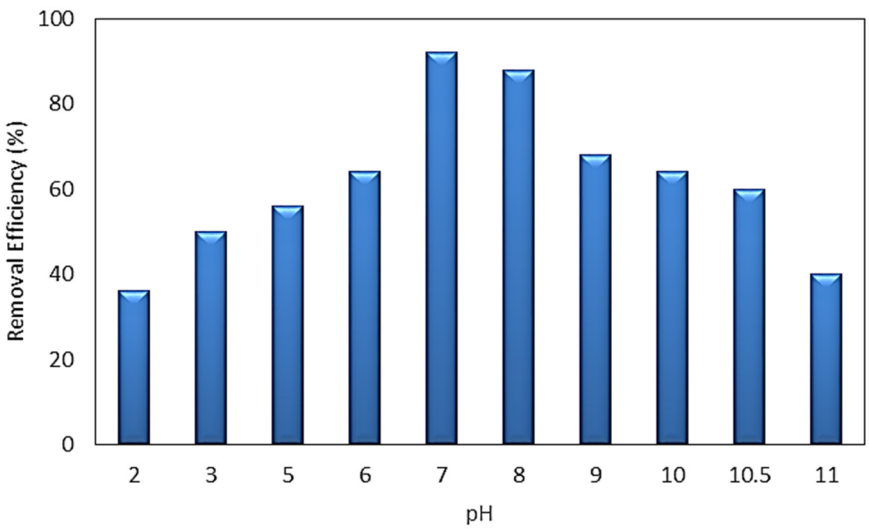

Fig. 6.The effect of pH on removal efficiency of 4-CP (contact time= 100 min, 4-CP concentration = 25 mg L^{-1})

removal of 4-CP was increased from 76% to 92%, with enhancement the catalyst dosage from 0.25 to 1 g L^{-1}. Then, a decrease was observed in 4-CP removal with an enhancement in catalyst dosage from 1 to 3 g L^{-1}. Thus, the catalyst dosage of 1g L^{-1} was selected for rest of experiments. Interestingly, a small amount of the catalyst had been effective in degrading a large amount of 4-CP in conformity

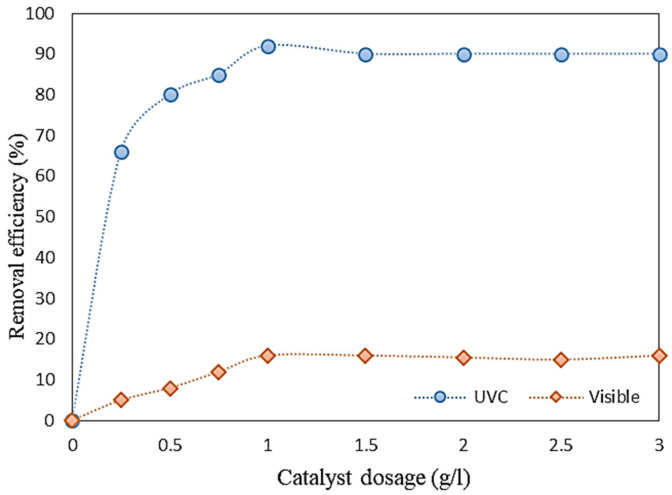

Fig. 7. The effect of the catalyst to remove the 4-CP by the UVC-La_2O_3 and Vis-La_2O_3 (pH =7, contact time= 100 min, 4-CP concentration = 25 mg L^{-1})

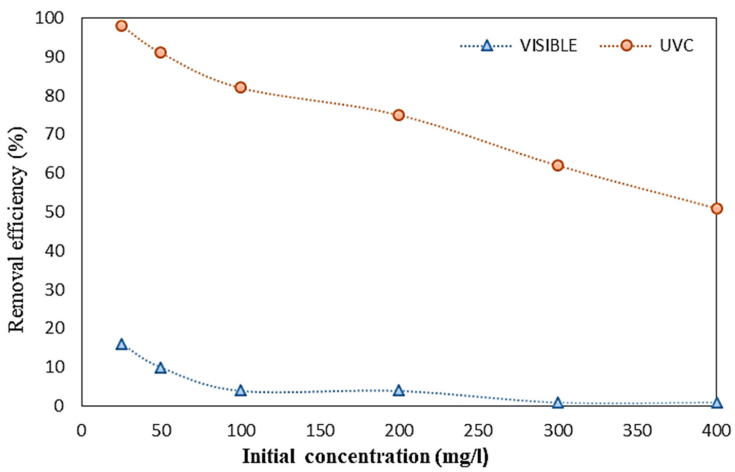

Fig. 8. The effect of initial concentration on the removal efficiency of 4-CP by the UVC-La_2O_3 and Vis-La_2O_3 (pH =7, catalyst= 1 g L^{-1}, contact time = 100 min)

with other results in the literature [37]. The photocatalytic activity of the catalysts strongly depends on surface properties, absorption properties, crystallinity and optical properties. The beneficial effect of La^{3+} increases with the efficient separation of photo-stimulated electrons and holes [46-49]. It has been reported that La^{3+} can act as photo source of electron traps [20, 46]. The initial rate of photocatalytic reactions was contribute to the mass of the catalyst. With increasing catalyst dosage, the surface area of the catalyst and the porosity were increased subsequently, the absorption and conversion rate was increased with increasing the surface area. However, at a certain value of the catalyst mass, the reaction rate was independent from catalyst Mass.This limitation is due to mass transfer and limitation of light penetration. When catalyst concentration increases, causes agglomeration (congestion), thus the catalytic particles are not available for photo absorption and the removal efficiency was declined [38, 39, 50]. Oxidized intermediates can react with diminishing species (eg, electrons) and decrease the rate of substrate degradation by decreasing the phenol contact efficiency [51]. Results of this study was correspond with other studies [38, 39, 41, 43, 51].

Effect of initial concentration

Fig. 8 indicate that removal efficiency of 4-CP by UVC-La_2O_3 process. Removal efficiency was reduced by increasing the initial concentration of

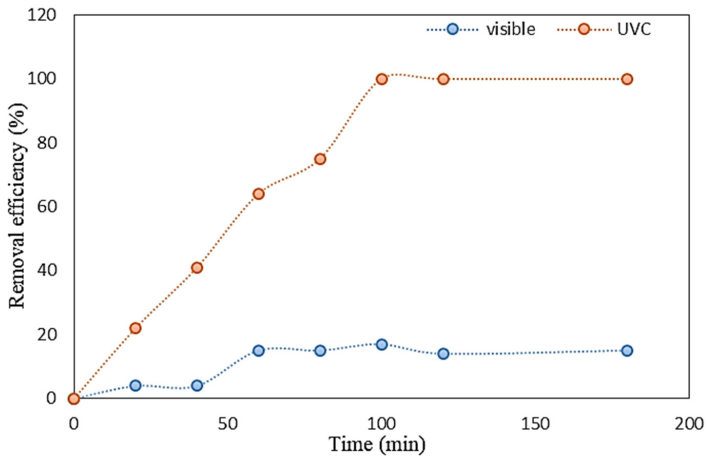

Fig. 9. The effect of contact time on the removal efficiency of 4-CP by the UVC-La_2O_3 and Vis-La_2O_3 (pH=7, catalyst dosage= 1 g L^{-1}, 4CP concentration = 25 mg L^{-1})

4-CP. Highest 4-CP removal (98%) was observed at the initial concentration of 25 mg L^{-1}. Then, a decrease was observed in removal efficiency of 4-CP with an increasing the initial concentration of 4-CP. Obviously, increasing the initial pollutant concentration would decrease the possibility of reaction between their molecules and those of reactant species. As the concentration of 4-CP increases, more and more reactant molecules are likely to flock together on the catalyst surface competing for the active sites among themselves. This decreases the oxidative conversion [37]. With increasing initial concentrations of 4-CP, the molecules absorption on the catalyst surface is increased, while the amount of hydroxyl Radical (OH*) remained constant. Thus, the number of available hydroxyl radicals to attack the molecules of 4-CP was dropped, and photocatalytic degradation efficiency is decline [38, 39]. With increasing concentrations of 4-CP, transfer path of photons to the catalyst surface has cut by molecules of 4-CP and reduce the absorption of photons on the catalyst surface. So, the efficiency of photocatalytic degradation (PCD) is reduce. This results is similar to the findings of previous studies [37-39, 41, 43, 52, 53].

Effect of contact time

The removal efficiency of 4-CP was studied at operational parameters including catalyst dosage (1g L^{-1}) pH=7, initial concentration (25 mg L^{-1}) and contact time of 20 -180 min for UVC-La_2O_3 and Vis-La_2O_3 processes (Fig. 9). At the reaction time of 20 to 60 min, removal efficiency of 4-CP by UVC-La_2O_3 process was increased from 24% to 64%, and then the reaction time was increased to 100 min and 120 min, removal efficiency increased to 100%. Therefore, the optimal time for the removal of 4-CP by the UVC-La_2O_3 process, the reaction time was 100 min. The removal efficiency of 4-CP by the Vis -La_2O_3 process on the range of 20-100 min was increased from 4% to 15% and then remained stable until 180 min. So, the reaction time of 100 min was selected for removal of the 4-CP by the Vis-La_2O_3. The oxidative degradation of 4-CP was enhanced if the reaction time was increased from 20 to 180 min. This phenomenon is due to enhancement of catalyst contact with the desired compound and subsequently enhancing decomposition with hydroxyl radicals produced from the catalyst and increasing the time of exposure to UV radiation and also produced high hydroxyl radicals [54, 55]. This result was agreed with other studies [37, 40, 54, 55].

Mineralization

Fig.10 shows the removal of organic material by measurement of COD and TOC at 20-180 min. 4-CP, COD and TOC removal rates were 100%, 65% and 80 %, respectively. According to the results, the mineralization at optimum conditions was 20%. 4-CP and TOC removal efficiency difference due to metabolites was produced by decomposition of 4-CP. The AOS index was measured before the UVC/Vis-La_2O_3 and after the process UVC/Vis-La_2O_3 are presented in Fig. 11 The average oxidation state (AOS) was considered as useful parameter to determine the oxidation degree of mixed solutions as well as providing indirect information about the possibility of degradation (Eq.2) [26, 29, 30, 56].

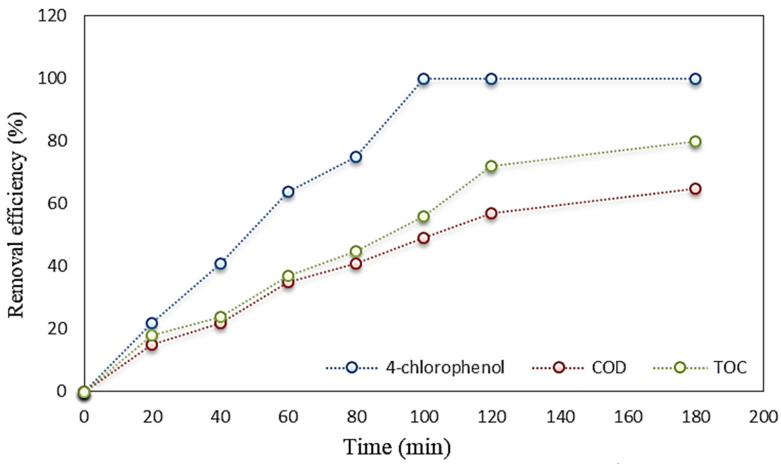

Fig. 10. Removal efficiency of 4-CP, TOC and COD by the UVC/Vis-La_2O_3

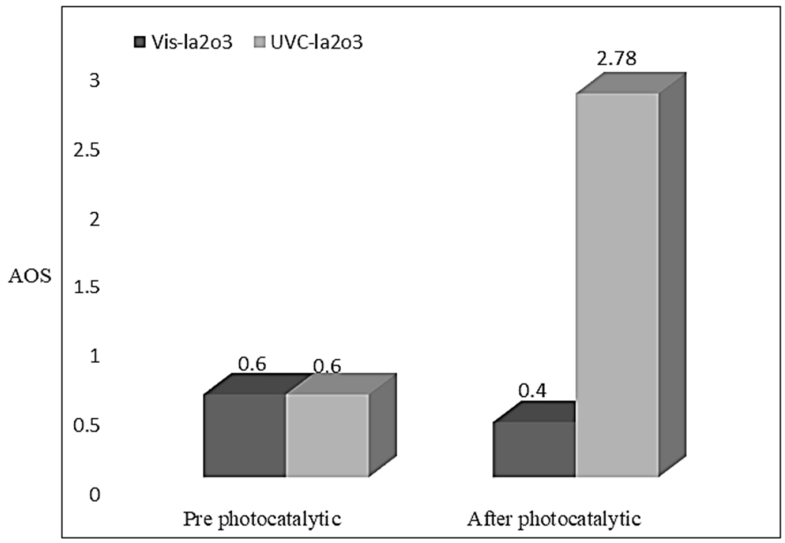

Fig. 11. AOS index measured before the UVC / Vis-La_2O_3 and after the process UVC/Vis-La_2O_3

$$AOS = 4 - 1.5\frac{COD}{TOC} \quad (2)$$

The range of AOS can be varied between +4 and -4. AOS = 4 is means of the most oxidized form of carbon and it is belong to the carbon dioxide. AOS = -4 is ascribe to the methan which is the most reduced form of carbon [57]. In this study, the AOS before the process and under process optimization (pH =7, La_2O_3= 1 g L^{-1} and reaction time 60 min) was measured +0.6 and +2.78, respectively. So, AOS indices was showed an increasing trend of mineralization. In other words, the process of degradation of 4-CP was improved with photocatalytic degradation by UVC-La_2O_3.

Adsorption effect

In heterogeneous catalytic degradation systems, the adsorption of both pollutants and intermediates can be occurred effectively and has a remarkable effect on the performance of process. For this purpose, we evaluated the proportion of 4-CP removal through adsorption on La_2O_3, since solid photo-catalyst used in this study can act as adsorbent for removal of contaminants [58]. The experiment with no irradiation denotes for adsorption effect on the 4-CP removal efficiency as well as activation of photo-catalyst through UVC/Vis irradiation. Adsorption experiments in dark conditions were carried out in the same conditions as selected levels

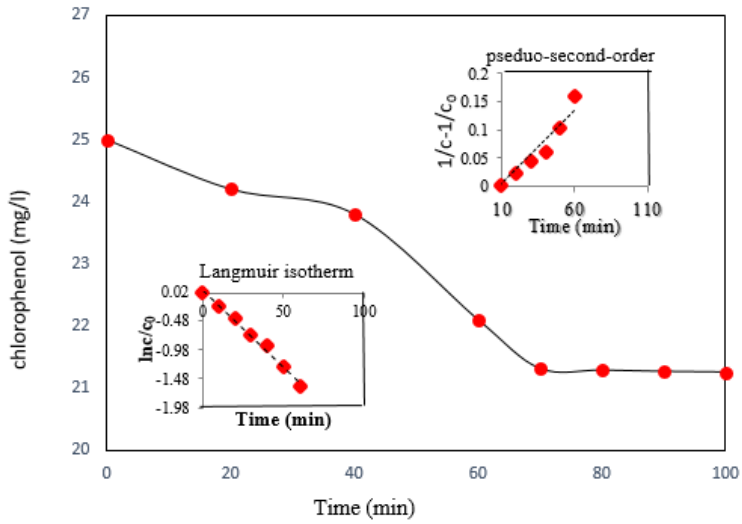

Fig. 12. Adsorption of 4CP on La_2O_3 within 100 min at initial 4CP: 25 mg L^{-1}.

of operational parameters (pH=7, catalyst dosage= 1 g L^{-1}, 4-CP concentration = 25 mg L^{-1}) to calculate the equilibrium of the adsorption process. The adsorption rate was moderate and equilibrium status was obtained around 100 min and no significant change was observed for longer contact times (Fig. 12). Investigation of isotherm models of adsorption process was carried out for 4-CP adsorption. The experimental data of adsorption equilibrium were investigated using Langmuir and pseudo- second order models. The linear forms of isotherm and kinetic models are as follows [58, 59]:

$$\frac{C_e}{q_e} = \left(\frac{1}{K_L Q_m}\right) + \left(\frac{1}{Q_m}\right) C_e \quad (Langmuir\ isotherm) \tag{3}$$

$$\frac{t}{q_t} = \left(\frac{1}{k_2 q_e^2}\right) + \left(\frac{1}{q_e}\right) t \quad (Pseudo-second-order) \tag{4}$$

Where q_e is the amount of adsorbed at equilibrium time (mg G^{-1}), qt is the amount of adsorbed at the time of t, Ce is the equilibrium concentration of the contaminant in the solution (mg L^{-1}), K_L is the Langmuir constant (l Mg^{-1}), and K_f and n are the Ferunlich constants. It is obvious that the 4-CP removal adsorption on La_2O_3 nanoparticles was consistent with Langmuir model (R^2 > 0.99). The maximum monolayer adsorption capacity was found to be 3.75 mg G^{-1} according to the Langmuir isotherm, suggesting that La_2O_3 nanoparticles has low adsorption capacity for the adsorption of pollutants.

Reaction mechanism

During photocatalytic degradation of 4-CP by catalyst, the intermediate metabolites produced by advanced 4-CP oxidation can include: hydroquinone (HQ), benzoquinone (BQ), 4-chloroectocol (4-cc), hydroxylhydroquinone (HHQ), hydroxybenzoquinone (HBQ), trihydroxybenylene (TBP). Chlorophenol is oxidizes to HQ and HQ oxide for the first time and then oxidizes to HHQ. Eventually, HHQ is convert to CO_2. Radical hydroxyl in the presence of soluble oxygen can be generated by the following reactions [41]:

$$H_2O + h^+ \rightarrow OH^{\bullet} + H^+ \tag{5}$$

$$O_2 + e^- \rightarrow O_2^{\bullet -} \tag{6}$$

$$2H_2O + O_2^{\bullet -} \rightarrow 2H_2O_2 \tag{7}$$

$$H_2O_2 \rightarrow 2OH^{\bullet} \tag{8}$$

In the absence of oxygen, small amount of radical hydroxyl is produced only from equation [3]. As a result, the HQ oxidation rate is reduced to HHQ. In the presence of a mild oxidizing agent, oxidation from HQ produces BQ, which is a reversible reaction. As shown in Fig. 13, there is a small amount of HHQ, while the HQ and BQ concentrations are relatively constant. Accordingly,

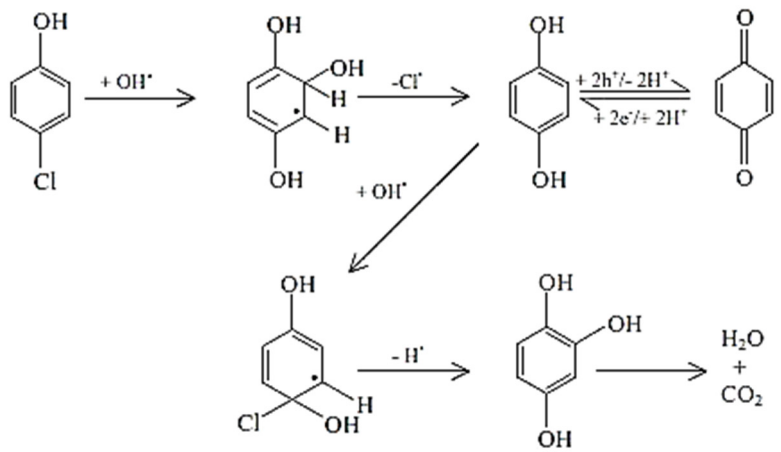

Fig. 13. Reaction pathway for photocatalytic degradation of 4-CP in the presence of soluble oxygen

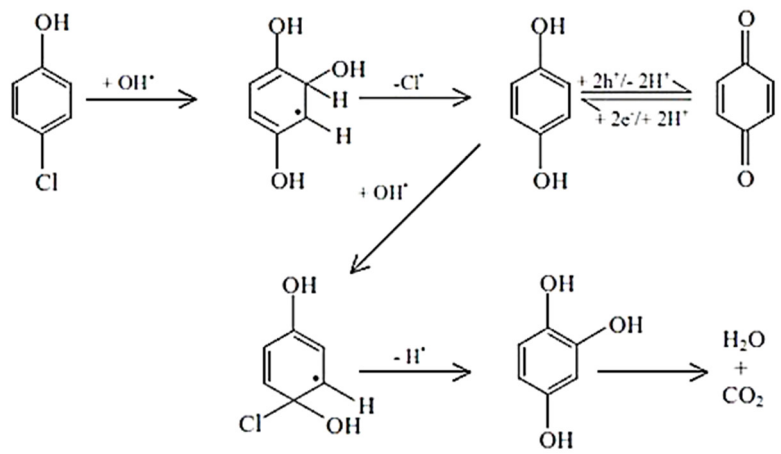

Fig. 14. Reaction pathway for photocatalytic degradation of 4-CP in the absence of oxygen dissolution

the proposed pathway for photocatalytic degradation of 4-CP in the absence of oxygen is shown in Fig. 14 [41].

Kinetics of photocatalytic removal of 4-CP

Several studies had shown that photocatalytic rate can be described using pseudo first-order kinetics. The plot of Ln (C/C_0) vs. reaction time provided a linear relationship (Fig. 15). Accordingly, the kinetics of photocatalytic degradation of organic compounds are follow a pseudo linear kinetic equation which is as follows:

$$Ln\frac{C}{C_0} = k_{app}t \qquad (9)$$

Where, C_0, C_t are initial and residual 4-CP concentrations (mg L^{-1}) at specified reaction time t (min), respectively and K_{app} is apparent reaction rate constant. Among the kinetic models, the pseudo-first order model due to the highest correlation coefficient of R^2 = 0.991 for the La_2O_3-UVC process (Fig. 15).

Reusability performance of photo-catalyst

In practical applications, reusability is a paramount factor for appraising the economical and applicability of catalyst. To assess the reusability of La_2O_3 photo-catalyst in degradation process, its capability was examined in five consecutive experimental runs at the same operational conditions and the results are

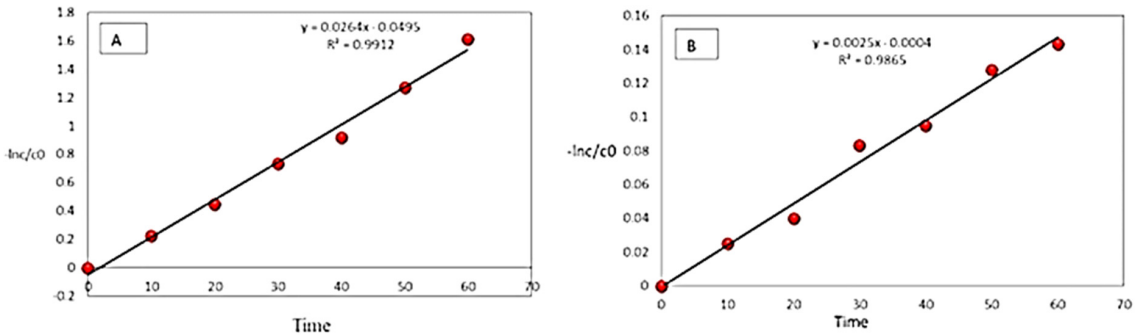

Fig. 15. Pseudo-first order kinetic model for the removal of 4-CP (a) UVC-La_2O_3 process, (b) Vis-La_2O_3 process

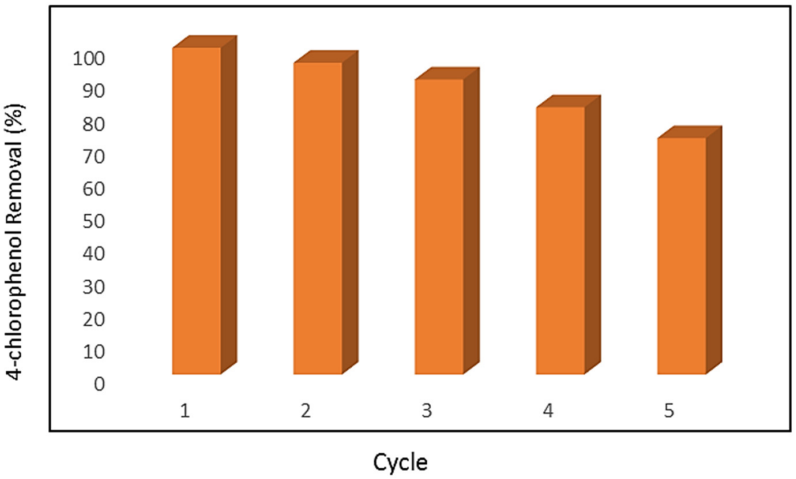

Fig. 16. Reusability of La_2o_3 in La_2O_3/UVc system within five consecutive experimental cycles under optimum conditions (initial La_2O_3 dosage: 0.7 g L^{-1}, initial 4-CP: 25 mg L^{-1}, reaction time: 100 min

illustrated in Fig. 16. After each experimental cycle, the spent La_2O_3 was chemically recovered using 0.2 M H_2SO_4 solution within 45 min. As shown in Fig. 16, the 4-CP removal rates at the first, second, third, fourth and fifth cycles were found to be 100, 95.4, 90.3, 81.8 and 72.35%, respectively. Consequently, the loss in the 4-CP removal over La_2O_3 system after fifth cycles was about 27.65%, confirming that La_2O_3 can be considered as a recoverable and efficient catalyst with the high reusability potential. Catalytic activities of La_2O_3 may be decreased due to increase competition between intermediates and parent compounds for reacting with radicals after each cycle and also deactivation of active sites on the catalyst surface during washing and drying processes. Another reason might be associated with the reduction of surface area and subsequently decreasing the adsorption capacity of catalyst via blocking the pores of the catalyst surface by pollutants and/or by-products. Furthermore, the regeneration of catalyst may result in the loss of La_2O_3 quantity from the zeolite support surface as well as fouling of the sonocatalyst surface by the big organic intermediate molecules [58].

CONCLUSION

This study presented the removal efficiency of 4-CP from aqueous solutions using lanthanum oxide in the presence of UVC/Vis radiation. Highest removal efficiency of 4-CP was observed at pH =7. Result was indicated that the removal of 4-CP was increased from 76% to 92%, with enhancement the catalyst dosage from 0.25 to 1 g L^{-1}. Then, a decrease was observed in 4-CP removal with an enhancement in catalyst dosage from 1 to 3 g L^{-1}. Highest 4-CP removal (98%) was observed at the initial concentration of 25 mg L^{-1}. At the contact time from 20 to 60 min, removal efficiency of 4-CP was increased from 24% to 64%,

respectively. The contact time was increased to 120 min, removal efficiency of 4-CP was increased to 100%. Therefore, the optimal reaction time was 100 min. The AOS indices was showed an increasing trend of mineralization. In other words, the process of degradation of 4-CP was improved with photocatalytic degradation by UVC-La_2O_3. Among the kinetic models, the pseudo-first order model due to the highest correlation coefficient of R^2 = 0.991 for the La_2O_3-UVC process.

ACKNOWLEDGEMENT

This paper is issued from the thesis with contact number of ETRC-9333. Special thanks to Ahvaz Jundishapur University of Medical Sciences for the financial support.

CONFLICT OF INTEREST

The authors declare that there is no conflict of interests regarding the publication of this manuscript.

REFERENCES

1. Hidalgo AM, León G, Gómez M, Murcia MD, Gómez E, Gómez JL. Application of the Spiegler–Kedem–Kachalsky model to the removal of 4-chlorophenol by different nanofiltration membranes. Desalination. 2013;315:70-5.
2. De Rooij C, Defourny C, Thompson RS, Garny V, Lecloux A, Van Wijk D. 1,1,1-Trichloroethane Marine Risk Assessment with Special Reference to the Osparcom Region: North Sea. Environmental Monitoring and Assessment. 2004;97(1-3):39-56.
3. Bacardit J, García-Molina V, Bayarri B, Giménez J, Chamarro E, Sans C, et al. Coupled photochemical-biological system to treat biorecalcitrant wastewater. Water Science and Technology. 2007;55(12):95-100.
4. CİFcİ DİZ, GÜNeŞ E, GÜNeŞ Y. Treatment of Dye-producing Chemical Industry Wastewater by Persulfate Advanced Oxidation. Environmental Research and Technology. 2020.
5. Igbinosa EO, Odjadjare EE, Chigor VN, Igbinosa IH, Emoghene AO, Ekhaise FO, et al. Toxicological Profile of Chlorophenols and Their Derivatives in the Environment: The Public Health Perspective. The Scientific World Journal. 2013;2013:1-11.
6. Pozan GS, Kambur A. Removal of 4-chlorophenol from wastewater: Preparation, characterization and photocatalytic activity of alkaline earth oxide doped TiO_2. Applied Catalysis B: Environmental. 2013;129:409-15.
7. Lin J-G, Chao AC, Ma Y-S. Removal of 2-Chlorophenol from Wastewater with the Ultrasonic/Fenton Process. Proceedings of the 52nd INDUSTRIAL WASTE CONFERENCE May 5–7, 1997: CRC Press; 2020. p. 355-67.
8. Wang N, Li X, Wang Y, Quan X, Chen G. Evaluation of bias potential enhanced photocatalytic degradation of 4-chlorophenol with TiO_2 nanotube fabricated by anodic oxidation method. Chemical Engineering Journal. 2009;146(1):30-5.
9. Gholizadeh A, Kermani M, Gholami M, Farzadkia M, Yaghmaeian K. Removal Efficiency, Adsorption Kinetics and Isotherms of Phenolic Compounds from Aqueous Solution Using Rice Bran Ash. Asian Journal of Chemistry. 2013;25(7):3871-8.
10. Lücking F, Köser H, Jank M, Ritter A. Iron powder, graphite and activated carbon as catalysts for the oxidation of 4-chlorophenol with hydrogen peroxide in aqueous solution. Water Research. 1998;32(9):2607-14.
11. Lettmann C, Hildenbrand K, Kisch H, Macyk W, Maier WF. Visible light photodegradation of 4-chlorophenol with a coke-containing titanium dioxide photocatalyst. Applied Catalysis B: Environmental. 2001;32(4):215-27.
12. Jorfi S, Ghaedrahmat Z. Evaluating the efficiency of advanced oxidation processes for textile wastewater treatment: Electro-kinetic, sonochemical and persulfate. Environmental Progress & Sustainable Energy. 2020;40(2).
13. Rahmat ZG, Ahmadi M. Activation of persulfate by Fe^{2+} for saline recalcitrant petrochemical wastewater treatment: Intermediates identification and kinetic study. DESALINATION AND WATER TREATMENT. 2019;166:35-43.
14. Hu R, Li C, Wang X, Sun Y, Jia H, Su H, et al. Photocatalytic activities of $LaFeO_3$ and La_2FeTiO_6 in p-chlorophenol degradation under visible light. Catalysis Communications. 2012;29:35-9.
15. Eskandari N, Nabiyouni G, Masoumi S, Ghanbari D. Preparation of a new magnetic and photo-catalyst $CoFe_2O_4$–$SrTiO_3$ perovskite nanocomposite for photo-degradation of toxic dyes under short time visible irradiation. Composites Part B: Engineering. 2019;176:107343.
16. Naghikhani R, Nabiyouni G, Ghanbari D. Simple and green synthesis of $CuFe_2O_4$–CuO nanocomposite using some natural extracts: photo-degradation and magnetic study of nanoparticles. Journal of Materials Science: Materials in Electronics. 2017;29(6):4689-703.
17. Samarghandi MR, Rahmani AR, Samadi MT, Kiamanesh M, Azarian G. Degradation of Pentachlorophenol in Aqueous Solution by the UV/ZrO_2/H_2O_2 Photocatalytic Process. Avicenna Journal of Environmental Health Engineering. 2015;In Press(In Press).
18. Neppolian B, Jung H, Choi H. Photocatalytic Degradation of 4-Chlorophenol Using TiO_2 and Pt-TiO_2 Nanoparticles Prepared by Sol-Gel Method. Journal of Advanced Oxidation Technologies. 2007;10(2).
19. Saffarzadeh S, Nabiyouni G, Ghanbari D. Preparation of $Ni(OH)_2$, NiO and $NiFe_2O_4$ nanoparticles: magnetic and photo-catalyst $NiFe_2O_4$–NiO nanocomposites. Journal of Materials Science: Materials in Electronics. 2016;27(12):13338-50.
20. Alimoradzadeh R, Assadi A, Nasseri S, Mehrasbi MR. Photocatalytic degradation of 4-chlorophenol by UV/H_2O_2/NiO process in aqueous solution. Iranian Journal of Environmental Health Science & Engineering. 2012;9(1).
21. Parida KM, Naik B. Synthesis of mesoporous $TiO_{2-x}N_x$ spheres by template free homogeneous co-precipitation method and their photo-catalytic activity under visible light illumination. Journal of Colloid and Interface Science. 2009;333(1):269-76.
22. Moradi B, Nabiyouni G, Ghanbari D. Rapid photo-degradation of toxic dye pollutants: green synthesis of mono-disperse Fe_3O_4–CeO_2 nanocomposites in the presence of lemon extract. Journal of Materials Science:

Materials in Electronics. 2018;29(13):11065-80.
23. Etminan M, Nabiyouni G, Ghanbari D. Preparation of tin ferrite–tin oxide by hydrothermal, precipitation and auto-combustion: photo-catalyst and magnetic nanocomposites for degradation of toxic azo-dyes. Journal of Materials Science: Materials in Electronics. 2017;29(3):1766-76.
24. Sheng J, Zhang S, Lv S, Sun W. Surfactant-assisted synthesis and characterization of lanthanum oxide nanostructures. Journal of Materials Science. 2007;42(23):9565-71.
25. Cao G, Li Y, Zhang Q, Wang H. Synthesis and characterization of $La_2O_3/TiO_{2-x}F_x$ and the visible light photocatalytic oxidation of 4-chlorophenol. Journal of Hazardous Materials. 2010;178(1-3):440-9.
26. Taherian S, Entezari MH, Ghows N. Sono-catalytic degradation and fast mineralization of p-chlorophenol: $La_{0.7}Sr_{0.3}MnO_3$ as a nano-magnetic green catalyst. Ultrasonics Sonochemistry. 2013;20(6):1419-27.
27. Li L, Wang X, Zhang Y. Enhanced visible light-responsive photocatalytic activity of $LnFeO_3$ (Ln=La, Sm) nanoparticles by synergistic catalysis. Materials Research Bulletin. 2014;50:18-22.
28. Moothedan M, Sherly KB. Synthesis, characterization and sorption studies of nano lanthanum oxide. Journal of Water Process Engineering. 2016;9:29-37.
29. Venkatachalam N, Palanichamy M, Murugesan V. Sol–gel preparation and characterization of alkaline earth metal doped nano TiO_2: Efficient photocatalytic degradation of 4-chlorophenol. Journal of Molecular Catalysis A: Chemical. 2007;273(1-2):177-85.
30. Stafford U, Gray KA, Kamat PV. Photocatalytic Degradation of 4-Chlorophenol: The Effects of Varying TiO_2 Concentration and Light Wavelength. Journal of Catalysis. 1997;167(1):25-32.
31. Selvam NCS, Narayanan S, Kennedy LJ, Vijaya JJ. Pure and Mg-doped self-assembled ZnO nano-particles for the enhanced photocatalytic degradation of 4-chlorophenol. Journal of Environmental Sciences. 2013;25(10):2157-67.
32. Wang K, Wu Y, Li H, Li M, Guan F, Fan H. A hybrid antioxidizing and antibacterial material based on Ag–La_2O_3 nanocomposites. Journal of Inorganic Biochemistry. 2014;141:36-42.
33. Hu C, Liu H, Dong W, Zhang Y, Bao G, Lao C, et al. $La(OH)_3$ and La_2O_3 Nanobelts — Synthesis and Physical Properties. ChemInform. 2007;38(17).
34. Shojaie A, Fattahi M, Jorfi S, Ghasemi B. Hydrothermal synthesis of Fe-TiO_2 -Ag nano-sphere for photocatalytic degradation of 4-chlorophenol (4-CP): Investigating the effect of hydrothermal temperature and time as well as calcination temperature. Journal of Environmental Chemical Engineering. 2017;5(5):4564-72.
35. Glaze WH, Kang JW. Advanced oxidation processes. Test of a kinetic model for the oxidation of organic compounds with ozone and hydrogen peroxide in a semibatch reactor. Industrial & Engineering Chemistry Research. 1989;28(11):1580-7.
36. Farias LA. Resumo de tese de doutorado. Revista Obutchénie. 2018:536-44.
37. Deka B, Bhattacharyya KG. Using coal fly ash as a support for Mn(II), Co(II) and Ni(II) and utilizing the materials as novel oxidation catalysts for 4-chlorophenol mineralization. Journal of Environmental Management. 2015;150:479-88.
38. Ram C, Dhir A, Kamboj M. STUDIES ON THE USE OF CALCIUM HYPOCHLORITE IN THE TiO2 MEDIATED DEGRADATION OF PHARMACEUTICAL WASTEWATER. Environmental Engineering and Management Journal. 2016;15(8):1713-20.
39. Ezerskis Z, Jusys Z. Oxidation of chlorophenols on Pt electrode in alkaline solution studied by cyclic voltammetry, galvanostatic electrolysis, and gas chromatographymass spectrometry. Pure and Applied Chemistry. 2001;73(12):1929-40.
40. Azzam MO, Al-Tarazi M, Tahboub Y. Anodic destruction of 4-chlorophenol solution. Journal of Hazardous Materials. 2000;75(1):99-113.
41. Moonsiri M, Rangsunvigit P, Chavadej S, Gulari E. Effects of Pt and Ag on the photocatalytic degradation of 4-chlorophenol and its by-products. Chemical Engineering Journal. 2004;97(2-3):241-8.
42. Zendehdel R, Tayefeh-Rahimian R, Kabir A. Chronic Exposure to Chlorophenol Related Compounds in the Pesticide Production Workplace and Lung Cancer: A Meta-Analysis. Asian Pacific Journal of Cancer Prevention. 2014;15(13):5149-53.
43. Kindsigo M, Hautaniemi M, Kallas J. Kinetic modelling of wet oxidation treated debarking water. Proceedings of the Estonian Academy of Sciences. 2010;59(3):233.
44. Yasuga. Int J Hematol. 1995;62:91.
45. Guittonneau S, Glaze WH, Duguet JP, Wable O, Mallevialle J. Characterization of Natural Water for Potential to Oxidize Organic Pollutants with Ozone. Ozone: Science & Engineering. 1992;14(3):185-96.
46. Xu H, Li H, Sun G, Xia J, Wu C, Ye Z, et al. Photocatalytic activity of La2O3-modified silver vanadates catalyst for Rhodamine B dye degradation under visible light irradiation. Chemical Engineering Journal. 2010;160(1):33-41.
47. Huo Y, Zhu J, Li J, Li G, Li H. An active La/TiO_2 photocatalyst prepared by ultrasonication-assisted sol–gel method followed by treatment under supercritical conditions. Journal of Molecular Catalysis A: Chemical. 2007;278(1-2):237-43.
48. Jia T, Wang W, Long F, Fu Z, Wang H, Zhang Q. Fabrication, characterization and photocatalytic activity of La-doped ZnO nanowires. Journal of Alloys and Compounds. 2009;484(1-2):410-5.
49. Anandan S, Vinu A, Sheeja Lovely KLP, Gokulakrishnan N, Srinivasu P, Mori T, et al. Photocatalytic activity of La-doped ZnO for the degradation of monocrotophos in aqueous suspension. Journal of Molecular Catalysis A: Chemical. 2007;266(1-2):149-57.
50. Peyton GR, Glaze WH. Destruction of pollutants in water with ozone in combination with ultraviolet radiation. 3. Photolysis of aqueous ozone. Environmental Science & Technology. 1988;22(7):761-7.
51. Nansheng D, Tao F, Shizhong T. Photodegradation of dyes in aqueous solutions containing Fe(II)-hydroxy complex I. Photodegradation kinetics. Chemosphere. 1996;33(3):547-57.
52. García-Molina V, López-Arias M, Florczyk M, Chamarro E, Esplugas S. Wet peroxide oxidation of chlorophenols. Water Research. 2005;39(5):795-802.
53. García-Molina V, Kallas J, Esplugas S. Wet oxidation of 4-chlorophenol. Chemical Engineering Journal. 2007;126(1):59-65.
54. Contreras EM. Optimización de los procesos de tratamiento biológico de efluentes industriales para la remoción de

carbono y nitrógeno: Universidad Nacional de La Plata.
55. Lipczynska-Kochany E. Degradation of nitrobenzene and nitrophenols by means of advanced oxidation processes in a homogeneous phase: Photolysis in the presence of hydrogen peroxide versus the Fenton reaction. Chemosphere. 1992;24(9):1369-80.
56. Adams VD. Water and Wastewater Examination Manual. Routledge; 2017.
57. Mantzavinos D. Assessment of partial treatment of polyethylene glycol wastewaters by wet air oxidation. Water Research. 2000;34(5):1620-8.
58. Jorfi S, Pourfadakari S, Kakavandi B. A new approach in sono-photocatalytic degradation of recalcitrant textile wastewater using MgO@Zeolite nanostructure under UVA irradiation. Chemical Engineering Journal. 2018;343:95-107.